Scanning gel electrochemical microscopy: Combination with quartz crystal microbalance for studying the electrolyte residue

Gustavo Adrián Echeveste Salazar, Mariela Alicia Brites Helú, Alain Walcarius, Liang Liu

Scanning gel electrochemical microscopy: Combination with quartz crystal microbalance for studying the electrolyte residue

Gustavo Adrián Echeveste Salazar, Mariela Alicia Brites Helú, Alain Walcarius, Liang Liu*

Université de Lorraine, CNRS, Laboratoire de Chimie Physique et Microbiologie pour les Matériaux et l'Environnement (LCPME), F-54000 Nancy, France

*E-mail: liang.liu@cnrs.fr; liang.liu@univ-lorraine.fr

Abstract

The residue of electrolyte is a main challenge for local electrochemical measurements based on spatially localized contact between the electrolyte and the sample surface, such as scanning droplet cell or scanning electrochemical cell microscopy. By immobilizing electrolyte in the form of gel, scanning gel electrochemical microscopy (SGECM) is expected to overcome this challenge. This work proposes an analytical method for studying the issue of electrolyte residue from gel probes in SGECM. It is based on measuring approach-retract curves of gel probes on a quartz crystal microbalance (QCM), where the resonance frequency is recorded and synchronized with the current response. Verified by SEM observation, the frequency shift after one approach-retract cycle is taken as a measure for systematically compare the extent of electrolyte residue on the Au-coated quartz crystal surface. The results show that the electrolyte residue from freshly prepared gel probes, especially after soaking redox probes, could be reduced to negligible after a few approach-retract cycles. It can also be

inhibited by co-electrodeposition of chitosan with tetraethoxysilane for preparing composite gel probe. Electrolyte residue could increase when over-pressing the gel against the sample. The residue of two types of gel probes and microcapillaries is also compared. The combination of QCM with SGECM offers a quality control method for gel probes before quantitative local electrochemical measurements.

Keywords

Scanning gel electrochemical microscopy, quartz crystal microbalance, electrolyte residue, microcapillaries, chitosan, tetraethoxysilane

1. Introduction

Scanning electrochemical probe techniques are powerful tools for studying electrochemical interfaces at micro and nanoscale. They can be divided in two categories: (1) localizing the electrode; (2) localizing the electrolyte. The former is known as scanning electrochemical microscopy, which is based on a micro or nano-electrode scanning over a sample that is immersed in liquid electrolyte [1]. The latter relies on spatially localized contact between the electrolyte and the sample. To achieve this, a common strategy is to contain the electrolyte in a micro or nano-capillary. The capillary, with a droplet hanging at its opening, is approached to the sample surface. As the droplet touches the sample, a local electrochemical interface is formed and electrochemical measurements can be carried out. The concept is known as scanning droplet cell (SDC). It could date back to 1980s where glass

capillaries or syringes were pushed against the sample to perform local electrochemical measurements, such as applying constant potential or current for local electrodeposition, or polarization and electrochemical impedance spectroscopy for studying localized corrosion [2,3]. Due to the limit of fabrication at that time, the spatial resolution was initially only in the range of hundreds of microns to millimetres.

Over the years, the spatial resolution of SDC has been significantly improved to a few microns and even nanometres, thanks to the technical development on the precise control of pulling capillaries (*e.g.* laser pullers mainly developed for electrophysiology). Recently, Mauzeroll's group has used SDC for studying localized corrosion of aluminium alloys and defects of diazonium modified glassy carbon electrodes [4,5]. A revolutionary progress in the field is scanning electrochemical cell microscopy (SECCM), which was developed by Unwin and co-workers [6]. Not only has the resolution entered nanometre range, the use of multi-barrelled capillaries also allowed electrochemical measurements to be done in three-electrode system in a nanosized droplet. The results can be easily compared with classical electrochemical measurements at macroscale. So far, SECCM has been used for studying grain boundaries [7], 2D nanomaterials [8–12], surfaces inhomogeneities [13–16], thin films [17–20] and electrochemical behaviour of single entities [21–29], as well as locally depositing catalyst particles [30].

SDC and SECCM have successfully pushed forward local electrochemical measurements to nanoscale. The key of the measurements is on the local wetting of

the electrolyte at the sample surface. While the shape of droplet at the opening of the capillary can be relatively well controlled by silanizing the walls, it may completely change once the drop wets the sample surface, depending on the local geometry and hydrophobicity of the sampling point. This was thoroughly discussed by Thatenhorst *et al.* [31], and calls for very careful experimental control. For example, covering the sample with an oil layer and locally piercing with capillary containing immiscible water-based electrolyte would greatly improve the quantitative control and reproducibility of the shape of wetting droplet [4,32]. The residue of electrolyte on the sample surface after measurement is another potential limit. It was experimentally confirmed by *ex-situ* SEM observation [33] as well as *in-situ* IR microscopy [34]. On one hand, this effect could be used to locate the sampling points for correlating with other characterizations, yet on the other hand one should avoid cross-interference from adjacent sampling points. In practice, the adjacent sampling points are usually set to several times the diameter of capillary opening. One effort to improve was to immobilize the electrolyte in the form of gel. This included replacing the liquid electrolyte by gel in SECCM [35], or depositing gel on electrodes which was referred as scanning gel electrochemical microscopy (SGECM) [36]. SGECM is based on a gel probe that is in soft contact with the sample surface for local electrochemical measurements, *e.g.* chronoamperometry, potentiometry and cyclic voltammetry [37–39]. Due to the soft nature of gel and absence of capillary, its shape can be modulated by pressing or stretching after touching the sample surface, offering the feature of flexible and tuneable spatial resolution. Although gel is generally accepted

to inhibit the electrolyte residue, it may still pose a risk especially when pressing against the sample surface. Therefore, like for SECCM, direct evidence on the electrolyte residue in SGECM is highly desired.

Considering the micrometer size of gel used in SGECM, one needs highly sensitive measurements for analyzing the quantity of potential electrolyte residue on the sample surface. This calls for quartz crystal microbalance (QCM), which is widely used for analysing small mass variations. The principle of QCM is monitoring the change in resonance frequency of the quartz crystal (QC) induced by tiny changes of the surface, such as deposition or dissolution of matters. The frequency change is then converted to mass change by physical models, such as those of Sauerbrey [40] and Kanazawa [41]. Due to the ease of measurement, QCM is often used as an *in-situ* monitoring tool for processes, such as thin film deposition, gel swelling and crystallization. It is also used for studying electrochemical processes (known as EQCM), including electrodeposition [42,43], electrochemical dissolution [44,45] and ion intercalation [46,47]. Moreover, EQCM is coupled with SECM to monitor the local change of QC electrodes as a result of micro-electrode induced redox reactions [48–50].

In this work, we integrated QCM with SGECM to study the residue of electrolyte from the gel probe upon contact with the sample surface. The results indicated that the frequency shift in QCM could qualitatively well reflect the electrolyte residue on the sample surface, as confirmed by SEM observations. It was observed that the fresh gel probes would need several approach-retract cycles to stabilize and prevent residue, which is in agreement with the phenomena in previous reports [37]. Pressing the gel

probe against the sample surface after touching may increase the residue of electrolyte due to the squeezing effect. The electrolyte residue is slightly more significant after soaking the gel probe in redox solution. Meanwhile, co-electrodeposition of chitosan with tetraethoxysilane (TEOS) would inhibit the residue of gel probes. This work confirmed the advantage of gel in immobilizing electrolyte as compared with scanning droplet-based techniques. Moreover, QCM may serve as a quality control tool for gel probes before SGECM measurements.

2. Experimental

2.1 Materials and chemicals

The probes were prepared with Pt wires of 25 and 100 μm diameter (99.9% purity, Goodfellow, UK). Borosilicate glass capillaries from Sutter Instruments were used for sealing the probes and making microcapillary probes. The former took BF 150-75-10 (Outer diameter (OD): 1.5 mm, Inner diameter (ID): 0.75 mm) and the latter took B 100-75-10 (OD: 1 mm, ID: 0.75 mm).

All the chemicals were used as received without further purification: chitosan (medium molecular weight, Aldrich), tetraethoxysilane (98%, Alfa-Aesar), glycerol (99%, Sigma), $NaNO_3$ (99%, Fluka), ferrocenedimethanol (98%, Aldrich), KCl (Merck), chlorotrimethylsilane (98%, Acros) and polyethylene glycol (PEG 2000, Merck).

2.2 Fabrication of probes

The gel probes were prepared by electrodeposition of chitosan on Pt micro-disk electrode (Type I), or by "electrodeposition + pulling" on etched Pt wires (Type II). Type I gel probes were fabricated by electrodeposition on a 25 µm diameter Pt micro-disk electrode with R_g (ratio between the diameter of the insulating shield and the microelectrode) between 2 and 3, from a 1:1 (*vol.* ratio) glycerol/H_2O solution containing 0.8 wt.% chitosan and 0.1 M $NaNO_3$. For co-electrodeposition of chitosan with tetraethoxysilane (TEOS), 21.3 µL of TEOS was added in 5 mL of the solution above, reaching TEOS concentration of 0.019 M. The electrodeposition was carried out by applying -0.95V *vs.* Ag/AgCl quasi-reference electrode (QRE) for 300 seconds. More details were reported in previous works [37,38].

Type II gel probes were prepared by "electrodeposition + pulling" following our previous work [39]. The process started with approaching an etched Pt wire (as working electrode (WE)) to the deposition solution with Ag/AgCl QRE and Pt wire counter electrode (CE). Once in contact (sensed by current feedback while applying -0.8V *vs.* Ag/AgCl QRE), the etched wire was immersed by 10 µm, held at -1 V *vs.* Ag/AgCl QRE for 1 s, and then withdrawn under the same potential at 3 µm/s until fully detached from the solution. The deposition solution consists of 1.5 wt.% chitosan, 1 wt.% polyethylene glycol and 0.125 M $NaNO_3$ in 1:1 (vol. ratio) glycerol/H_2O. The home-built "electrodeposition + pulling" setup consists of a potentiostat (PalmSens, The Netherlands) and a step motor (Owis, Germany) fully automated by a program written in VB.NET.

Microcapillary probes were fabricated by pulling borosilicate capillaries (OD 1.0 mm,

ID 0.75 mm) on a laser puller (P-2000, Sutter Instruments). The outer walls of the pulled capillaries were silanized by immersion in chlorotrimethylsilane with nitrogen gas flowing through the orifice. After silanization, the microcapillaries were filled with 1:1 (*vol.* ratio) glycerol/H_2O containing 1 mM ferrocenedimethanol and 0.05 M KCl. A 25 µm Pt wire was inserted in the electrolyte solution as RE/CE before electrochemical measurements. The typical images of Type I, Type II gel probes and microcapillary probe are shown in **Fig. 1**.

Figure 1

2.3 QCM coupled SGECM measurements

The QCM coupled SGECM measurements were carried out by integrating quartz crystal analyser (QCA 917, Princeton Applied Research) into a home-built SGECM setup as described before [38]. Standard 9 MHz AT-cut gold coated quartz crystals of 5 mm diameter were used. The oscillator circuit is configurated on a TTL-IC and with a stable oscillation function at heavy loads, offering an accuracy of 0.1 Hz and at a sample period of 0.1 s. The oscillation frequency from QCA, the current from potentiostat (PalmSens3, The Netherlands) and the piezo position from encoder (PI, Germany) were synchronized by the same ADC data acquisition card (PCI-2517, USA). The control program was written in VB.NET.

Approach-retract curves were performed to study the residue of electrolyte in SGECM and microcapillary-based measurements. The probes were approached to the QC sample surface at an average speed of 2 µm/s by current feedback at 0.4 V (E_{sample}

vs. E_{probe}), as described previously [39]. After touching the sample (normalized to z = 0), the Type II gel probe and the microcapillary were immediately retracted at the same speed. For Type I gel probe, it was also purposely pressed against the sample surface for different distance (2-10 μm) before retraction, taking advantage of the soft nature of the gel. During the measurement, the oscillation frequency shift was recorded together with the current as a function of vertical z position. Sequential measurements were also performed to examine the stability of the probes. They were carried out by repeating the approach-retract measurements in hopping mode with 50 μm lateral gap between adjacent sampling points.

2.4 Characterization of the samples

The samples after QCM-SGECM measurements were observed under optical microscope (Nikon, Japan) and further characterized by SEM (JEOL IT-500HR/LV, Japan). The composition of the contact area (after evaporation of solvent from the electrolyte residue) was analysed and mapped by EDX (Oxford Instruments, UK).

3. Results and discussion

The first step for any scanning probe technique is to approach the probe to the interaction range with the sample. For scanning electrochemical measurements with microcapillaries or gel probes, the most common and sensitive way to approach the probe is by current feedback [39,51], although other methods such as shear force were also used [36]. The concept is illustrated in **Fig. 2A**. A voltage signal (either in DC or

AC) is applied between the conductive sample and the electrode in the probe. When the probe is far from the sample, the circuit is open and only noise is recorded. Once the electrolyte in the probe touches the sample, the circuit is closed and a current spike is expected. From the instrumentation aspect, this spike is ideal for constructing closed-loop feedback. In this work, 0.4 V (E_{sample} *vs.* E_{probe}) DC voltage was applied for approaching all the probes. It was found to be sensitive enough, although Unwin and Koper [52] reported that AC signal could have even higher signal-to-noise ratio than DC signal for sensing the probe touching.

After touching, the probes are retracted away from the sample surface. Two scenarios are illustrated in **Fig. 2B**. Ideally, the gel probe immobilizes the electrolyte thus should not leave anything on the sample surface after measurement. **Fig. 2C** illustrates a typical approach-retract curve of a gel probe to the Au-coated QC surface, where both the current and frequency of QC are recorded by potentiostat and QCM, respectively. The current response is similar to our previous work [38]. A hysteresis is observed while retracting the probe, which reflects the adhesion between the gel and the QC sample. Interestingly, the frequency response of QC follows similar trend as the current hysteresis. It also shows a spike when the gel touches the sample, and then gradually restores to its initial value while retracting the probe. This confirms the adhesion during the retraction process. More importantly, the well synchronization of the current and QCM frequency signals for both touching and detaching show that QCM could be a promising tool for approaching gel probes to non-conductive surfaces. The detaching process is between a viscoelastic body (gel) and a rigid

surface (QC) (**Fig. 2B**, top). Thus, the decrease in frequency shift follows the same trend as the decrease in current, both reflecting the decrease in the contact area. After the gel probe completely detaches from QC surface, the current reduces to noise level, and there is no significant difference in the frequency response of the QC.

However, in reality the immobilization of electrolyte by the gel probe may be imperfect. This might yield the electrolyte leaving residue on the sample surface after approach-retract measurements. Here, a purposely overgrown gel is taken to study the effect of electrolyte residue, and the approach-retract curve is shown in **Fig. 2D**. Similar as **Fig. 2C**, both current and frequency can sensitively detect the touching of the probe with QC surface, and hysteresis is observed for retracting the probe. Nevertheless, the signals around the detaching position are quite different. The QCM frequency shift first decreases to almost zero, a position where the current starts to decrease from a plateau. Then, the frequency shift slightly increases to a stable value while the current decreases to zero (with noise). A hypothesis is that the detaching of gel probe involves two steps. The first step is the detaching between viscoelastic gel and rigid QC surface, resulting in a decrease in frequency shift. However, even the gel is already detached from QC, it may still stay in contact with the electrolyte residue, thus the current is still measurable. During this second step of detaching between gel and the electrolyte residue (**Fig. 2B**, bottom) (corresponds to the positions between the two dashed lines in **Fig. 2D**), the electrolyte residue reshapes, which might be the reason for a slight increase in frequency shift. Meanwhile, the current decreases due to the reduction in the contact area between the gel and electrolyte residue. This

hypothesis may explain the characteristic current and frequency change in approach-retract curves. Although the transient frequency response in detaching could be highly informative, its quantification is very complicated and beyond the focus of the current work. The position where the current decreases to zero (with noise) marks the complete detaching of the gel probe from the sample. At the same time, the QCM frequency shift also becomes almost constant, yet different from the initial value. This difference may be well explained by the presence of remaining liquid electrolyte from the gel probe on the QC surface.

Figure 2

As reported by Unwin's group, SEM can be used to observe the electrolyte residue after SECCM measurements to visualize the sampling points [33]. Here, the QC samples after approach-retract measurements of the gel probe are also examined by SEM after drying. **Fig. 3A** shows SEM image of a QC sample after two line-scans of measurements by fresh gel probes (respectively before (Line 1) and after (Line 2) soaking in ferrocenedimethanol). The residue of electrolyte on the sample surface is clearly visible for the first few measured spots. The spots gradually become smaller and invisible as the approach-retract cycle number increases. The phenomenon is consistent with our previous work, where highly reproducible approach-retract curves may only be measured after stabilizing fresh gel probes with several approach-retract cycles [38]. **Fig. 3B** represents the current and QCM frequency shift after the first sampling point with a gel probe freshly soaked in ferrocenedimethanol. A clear *ca.* 1.6 Hz frequency shift is observed, which corresponds to a large spot seen in SEM. For

the fifth sampling point, the frequency shift reduces to *ca.* 0.9 Hz (**Fig. 3C**), and the spot of remaining electrolyte also becomes smaller. When the spot becomes invisible, the difference in the frequency shift also becomes indifferentiable (**Fig. 3D**). The consistent results confirm the QCM frequency shift as a good indication for the electrolyte residue on the sample surface after approach-retract SGECM measurements. Note that EDX analysis were also attempted to characterize the spots, but there is no significant difference in C/Au ratio even for visible spots (Supporting Information **Fig. S1** and **S2)**, perhaps due to the limited sensitivity of measurements for such ultra-thin deposits. At the same time, when the electrolyte residue is clearly visible by *in-situ* QCM and *ex-situ* SEM, a position gap can be seen between the detaching point marked by current reducing to zero (with noise) and the point where the QCM frequency shift stabilises. The gap is denoted as ΔZ_{detach} in the later discussions (**Fig. 2** and **3**). It reduces as the electrolyte residue reduces, and becomes indifferentiable after the probe is stabilized from residue. This further confirms the trend in **Fig. 2** and could be explained by the two-step detaching hypothesis.

Figure 3

The results above clearly indicate that QCM is a reliable tool for measuring the electrolyte residue from gel probes on the sample surface. A straightforward evidence is the frequency shift of QC after detaching the gel probe, as shown in **Fig. 2** and **3**. This is directly linked to the quantity of electrolyte left on the QC before evaporation of solvent. Considering the shape of small droplets (as supported by SEM observations in **Fig. 3A**), one cannot use Sauerbrey's Equation for quantitative

analysis. Several reports attempted to analyse the frequency change induced by droplets in QCM based on modification of Kanazawa model, but their targeted droplets are much bigger in size as compared with our work [53]. Therefore, in this work, we keep using the frequency change after each approach-retract cycle as a measure for the extent of electrolyte residue but without over quantification (**Fig. 2** and **3**). Along with the QCM frequency shift, the current at contact point ($i_{contact}$) for each approach-retract sampling cycle is also presented (with the full approach-retract curves in Supporting Information **Fig. S3**, and **S4**). It mainly reflects the non-Faradaic behaviour of the contact, which indirectly suggests the contact area between gel and sample.

In the following sections, the effect of stabilization and squeezing, aging of precursor, as well as soaking electrolyte on the electrolyte residue from gel probes are systematically studied. An attempt to strengthen the gel probes by co-electrodeposition with TEOS is also demonstrated for reducing the electrolyte residue. Comparison among different types of gel probes and microcapillaries is also shown. A main advantage of QCM is that it could integrate to SGECM and serve as a tool for real-time quality control, as approach-retract curve on a known surface is anyway a necessary check for gel probes before measuring targeted samples. QCM measurements can also provide more direct information than SEM on the electrolyte residue, as the latter must be performed after drying the sample.

3.1 Gel probe stabilization.

Consistent with previous report [38], we systematically observed that the gel probes have to be stabilized by several approach-retract cycles before getting reproducible approach-retract curves. In the SEM image (**Fig. 3A**), it is clearly seen that the gel probe leaves visible traces on the QC surface in the first 5-6 sampling points before being stabilized. Thanks to the implementation of QCM, the extent of electrolyte residue can be semi-quantitatively measured by the frequency shift before and after each approach-retract cycle (**Fig. 2** and **3**). By repeating the cycle, the QCM frequency shift gradually reduces to zero (**Fig. 4 A**), which is in good agreement with the SEM observation (**Fig. 3A**). This confirms that the gel probes could reach a stable state without leaving any more electrolyte on the sample surface. This is in line with the trend of current at contact ($i_{contact}$), which also decreases in the first few cycles and then stabilizes (**Fig 4B**). From the full approach-retract curves (Supporting Information **Fig. S3A** and **S3B**), it is clearly seen that in the first few approach-retract cycles the detaching point gradually shifts towards the touching point, or in another word, the distance between touching and detaching decreases. After *ca.* 8-10 cycles, the approach-retract curves overlap, which further support the stabilization of the probe as seen from the QCM frequency shift. Moreover, the current at plateau during detaching also decreases before the gel probe gets stabilized. The physical meaning of this current remains a question as it originates from a mixture of interfacial electrochemical reactions with dynamic changing of the shape of gel (boundary for mass transport) and gel/sample contact, so we do not further discuss it in this work.

Soaking in electrolyte is a practical way to functionalize gel probes, *e.g.* by

impregnation with redox species. However, the gel probes will swell when immersing in an electrolyte even with the same solvent and ion concentration (compare insets in **Fig. 3A**), probably due to the change in retention factor of gel by the redox species. The freshly soaked probes would also naturally contain residue of free electrolyte. These yield much more significant residue on the sample in the first approach-retract measurements (compare Lines 1&2 in **Fig. 3A**). Correspondingly, the QCM frequency shift is also much higher compared with that for as-electrodeposited gel probes (**Fig. 4A**). The soaked gel probes could still be stabilized, as seen from the trend of frequency shift (**Fig. 4A**), $i_{contact}$ (**Fig. 4B**) and approach-retract curves (Supporting Information **Fig. S3C** and **S3D**), although it may take more approach-retract cycles. Practically, QCM can well indicate the stabilization of the gel probes during approach-retract cycles without the need to wait the electrolyte residue to evaporate and to pass the sample to SEM characterizations.

Figure 4

Let's remind that the gel probes are prepared by electrodeposition of chitosan on micro-disk electrodes. Due to the complexity of chitosan as a natural product, it is very difficult to prepare exactly the same deposition solution in different batches. Thus, the electrodeposition conditions need to slightly vary to adapt for obtaining gel probes with well controlled and reproducible shape. A practical way to avoid this is to keep using the same deposition solution for long time. But then a question arises: Does the aging of solution affect the properties of the gel? Comparing the inset photo of **Fig. 5A** with **Fig. 3A**, it is seen that the aging of solution does not visibly change

the shape of electrodeposited gel under the same deposition conditions. Nevertheless, QCM frequency shift indicates that the gel probes prepared from old precursor solution (15 days) have more residue of electrolyte in the first approach-retract cycles (**Fig. 5A**) as compared to gel probes prepared from the fresh precursor solution (**Fig. 4**). It also takes more approach-retract cycles to stabilize the probe. Here, the variation of $i_{contact}$ is less sensitive than QCM frequency shift upon stabilization (**Fig. 5B**). Nevertheless, one could still see the trend from approach-retract curves (Supporting Information **Fig. S4**), especially on the stabilization of "plateau" current during retract and the detach distance measured by current (ΔZ_i). The extent of residue, as measured from QCM frequency shift, is similar after soaking ferrocenedimethanol (**Fig. 5A**). The results probably suggest that the gel deposited from old precursor solution is less condense in structure, even though the apparent shape looks similar. This might be related to the poor stability of chitosan in solution [54,55] that increased the heterogeneity of deposits and altered the retention factor for ferrocenedimethanol. It is interesting that the detaching distance as measured by current (ΔZ_i) and QCM frequency shift (ΔZ_f)

Figure 5

From the current and QCM frequency shift, one may mark the *z* position of detaching by current reducing to zero (with noise) or by frequency shift getting stabilized. Deducted by the touching position which is normalized to zero, the detaching distance can be measured, denoted as ΔZ_i from current and ΔZ_f from frequency shift. It is clearly seen that both ΔZ_i and ΔZ_f decreases in the first few approach-retract cycles and

then stabilizes (Supporting Information **Fig. S5**), which agrees with the trend of stabilization as seen from **Fig. 4** and **5**. Note that the physical meaning of the detaching distance is still not fully clear. It may be affected by the viscoelasticity of the gel, the adhesion between gel and sample, as well as eventually the interfacial tension between gel and the electrolyte residue. Besides, the determination of ΔZ_f could also be inaccurate due to the difficulty in identifying the plateau, *e.g.* **Fig. 2D**. Therefore, it is pre-matured to make quantitative analysis and comparison, and this shall be further explored in future work.

3.2 Reinforcement of the gel probe by co-electrodeposition with TEOS

It is systematically seen from the results above that freshly prepared gel probes leave electrolyte on the sample surface during the first approach-retract cycles. Apart from stabilizing it by repeating the cycles while monitoring with QCM, another effort is made to mechanically reinforce the gel probes to reduce their swelling and thus the electrolyte residue. A common approach is to form inorganic-organic hybrid matrix.

TEOS is a promising precursor for this purpose. It has been intensively reported that TEOS-based sol-gel-derived silica could co-deposit with chitosan, improving the mechanical properties of the obtained composite gel [56–58]. More importantly, TEOS could also be electrodeposited under similar conditions as chitosan. In the mild acidic precursor, TEOS is in hydrolysed form (*i.e.*, $Si(OH)_4$), and by applying cathodic potential the local pH at the electrode increases yielding the condensation of silanol moieties [59,60]. This could perfectly match the electrodeposition of chitosan which is also based on the local modulation of pH near the cathode. Here, TEOS was

added in the chitosan deposition solution and co-electrodeposition was realized as verified by the Si/C ratio from EDX (Supporting Information **Fig. S6**).

Fig. 6A shows the QCM frequency shift of gel probes from co-electrodeposition of chitosan with TEOS (denoted as chitosan-TEOS probe). Only slight shift of frequency is observed for the first two approach-retract cycles of the chitosan-TEOS probe. Afterwards, the frequency shift is negligible considering the signal drift and accuracy of QCM. This suggests a clear improvement in immobilizing electrolyte as compared with chitosan-only gel probes. Moreover, the chitosan-TEOS probe is also prepared from a 15 days aged precursor. It is clearly seen that the frequency shift becomes much higher, and it is still instable even after 15 approach-retract cycles (**Fig. 6A**). This is likely because TEOS is already polymerized in the aged precursor *via* condensation, which is known to be unfavourable for electrodeposition [61,62]. In **Fig 6B**, it is seen that $i_{contact}$ for the chitosan-TEOS probes prepared from old precursor solution is similar to that for chitosan-only probes, but the chitosan-TEOS probes electrodeposited from fresh precursor had much lower $i_{contact}$. It is likely suggesting that the probe had much lower conductivity, which is in line with the mechanical reinforcement yielding less electrolyte residue. The complete approach-retract cycles current response curves are shown in Supporting Information **Fig. S7**. These results suggest that the electrolyte residue could be reduced by reinforcing chitosan gel probes *via* co-electrodeposition with TEOS, although the conductivity of gel might also be reduced as consequence. In practice, further optimizations are desired to achieve balanced performance of mechanical strength and ionic conductivity. Like for

chitosan-only system, aging of precursor for long time shall be avoided.

Figure 6

3.3 Squeezing effect

As discussed in our previous work [38], one major advantage of SGECM is the soft contact between the gel probe and the sample surface, which allows the gel probe to be purposely pressed or retracted after touching the sample. This would alter the contact area and bring an important feature of flexible resolution for local electrochemical measurements. Especially, when the gel probe is pressed against the sample, a risk of squeezing the gel and leaving free electrolyte over sample surface can be envisaged.

Fig. 7 shows a typical frequency shift variation curve during approaching-compressing-retracting a Type I chitosan gel probe, where the gel probe is pressed for 6 μm after touching the sample. After a spike at touching point, the frequency shift continues to increase almost linearly while the gel probe is pressed against the sample. During the retraction, the frequency shift gradually restores until the gel probe is fully detached from the sample. This transient frequency change of QC is interesting and may suggest the mechanical properties of the gel, yet the analysis is beyond the focus of this work. Here, we focus on the frequency shift after a complete approach-compress-retract cycle.

Figure 7

Fig. 8A shows the frequency shift after retracting the stabilized probes from a vertical

position where it is pressed for different distance against the QC. It is seen that for all the probes, *i.e.*, the chitosan-only probe, the chitosan probe soaked with ferrocenedimethanol, and the chitosan-TEOS probe, the frequency shift increases as the pressing distance increases. When pressing the probes "gently" for a small distance (< 6 μm), it is seen that the probe soaked with ferrocenedimethanol shows more electrolyte residue than that before soaking. This is in line with the results in **Fig. 4**, indicating that the gel is loosened by soaking in electrolyte solution. Meanwhile, co-electrodeposition with TEOS would enhance the mechanical properties of the gel and thus inhibit the electrolyte residue. The difference in frequency shift becomes minor when deeply pressing the gel up to 10 μm. Note that the height of a gel probe is usually around 30 μm. That being said, pressing for 10 μm is equivalent to squeezing the gel by *ca.* 30%, which is very harsh for the probe and rarely used in SGECM measurements. The gel probes prepared from aged precursor solutions leaves much more residue upon pressing than those prepared from fresh solutions (Supporting Information **Fig. S8**). This confirms that aging of deposition solutions is unfavourable for preparing gel probes.

Figure 8

Here, it is more difficult to pick the current for comparison. During an approach-retract cycle, after the gel probe touches the sample, the current response initially decreases regardless of the direction of movement of the probe (pressing as shown in **Fig. 7** or retracting in all previous figures). This is likely because of the non-Faradaic current. Thus, in the experiments shown in this work, the current

response after contact is a mixture of time (for non-Faradaic contribution) and shape (change of gel boundary and gel/sample contact area) effect. This could explain that the current at different compression distance is similar in **Fig. 8B**, as the decrease in non-Faradaic current with time could be compensated by the increase in Faradaic current due to the decrease in microelectrode-sample distance and increase in gel/sample contact area. Moreover, the dynamic shape change of gel even adds to the complexity by introducing viscoelastic effect. Thus, we would avoid over elaboration and discussion of the trend in current.

3.4 Comparison among different probes

Apart from the Type I gel probe that is relatively well studied [37,38], another type of gel probe (Type II) prepared by "electrodeposition + pulling" was recently also reported for carrying out local electrochemical measurements [39]. With the established method by QCM, we compare the electrolyte residue among these two types of gel probes as well as classical microcapillary probes.

Fig. 9A illustrates the frequency shift with the number of approach-retract cycles for Type I, Type II and microcapillary probes with diameter of contact *ca.* 25 μm (full approach-retract curves in Supporting Information **Fig. S9)**. It is seen that both Type I and Type II gel probes have a slight frequency shift in the first experiments, but the shift gradually decreases to almost zero after 5-6 cycles. The contact current $i_{contact}$ follows a similar trend (**Fig. 9B**). Meanwhile, the microcapillary with similar size of droplet has much higher frequency shift, indicating that it leaves much more electrolyte on the QC surface. Moreover, the frequency shift keeps almost constant

over approach-retract cycles, which is trivial as the electrolyte is not immobilized and will keep leaving on the sample surface. The residue is also clearly visible by optical microscope (Supporting Information **Fig. S10**). It is interesting that $i_{contact}$ appears to be stable over experiments (**Fig. 9B**). This suggests that if the surface tension of the sample is homogeneous over the surface (presumably the case here), the electrolyte residue could be stable (**Fig. 9A**) and may not affect the current measurement (**Fig. 9B**), which agrees with the observations by Unwin *et al* [51,52,63,64]. The results confirm the advantage of SGECM in immobilizing electrolyte and preventing residue, which would be useful for non-destructive quantitative analysis. As in previus cases, full current response of approach -retract cycles is presented in Supporting Information **Fig. S11**.

On the other hand, it should be noted that in practical applications, Type II and microcapillary probes can be fabricated to reach much smaller size of contact with the sample, as shown in inlet **Fig. 9C**. This could significantly improve the spatial resolution of local electrochemical measurements. The frequency shift for Type II gel probe with 3-5 μm diameter of contact is almost negligible even from the first experiment (**Fig. 9C**). The microcapillary probe of 1-2 μm opening also shows much less electrolyte residue as compared with that of 25 μm, yet the frequency shift is still visible over the experiments. The $i_{contact}$, not surprisingly, is also much lower than the probes with larger area of contact or opening, and is stable over experiments (**Fig. 9D**). The results suggest that the absolute quantity of electrolyte residue after an approach-retract experiment can be reduced by reducing the size of the gel or droplet

for Type II or microcapillary probes, respectively. Nevertheless, it does not mean that the extent of residue is reduced as it is relative to the contact area, even though the electrolyte residue may not interfere the current measurement if the sample is homogeneous in surface tension.

Figure 9

4. Conclusion

In summary, the integration of QCM with SGECM setup allows tracing the frequency shift of QC samples during the approach-retract of the gel probes. The frequency shift after an approach-retract cycle indicates the absolute quantity of electrolyte residue on the QC surface, which is confirmed by SEM observation. Taking this as a semi-quantitative measure, the electrolyte residue from different gel probes is systematically studied. It is observed that the freshly prepared gel probes have electrolyte residue, especially after soaking redox probes, yet it can be reduced to be invisible (both from QCM frequency shift and SEM observation) after a few approach-retract cycles. This confirms that the gel probes shall be stabilized before serious SGECM measurements, which can also be verified by the reproducibility of approach-retract curve of current response. Aging of chitosan precursor would deteriorate the strength of gel and thus increase the electrolyte residue, while co-electrodeposition of chitosan with TEOS would reinforce the gel and reduce the residue of electrolyte although it might also reduce the conductivity. Over-approaching the gel would slightly increase the residue of electrolyte due to the

squeezing effect. The comparison among Type I and Type II gel probes with microcapillary probes indicates that gel probes have much less electrolyte residue than microcapillaries at the same contact area with sample, which can be explained by the immobilization of electrolyte in the gel. This work proposes a method of quality control for gel probes after preparation. Approach-retract on a QC surface can be foreseen as a standard protocol to ensure well stabilization and negligible electrolyte residue of gel probes before quantitative SGECM measurements.

Acknowledgement

We gratefully acknowledge financial support from CNRS MOMENTUM Project (2018-2020) and University of Lorraine for supporting the PhD study of Gustavo Adrián Echeveste Salazar. The platform of Spectroscopies and Microscopies of Interfaces (SMI) of LCPME is also acknowledged. We highly appreciate the assistance from Dr. Mathieu Etienne in “reviving” the QCM.

References

[1] A.J. Bard, F.R.F. Fan, J. Kwak, O. Lev, Scanning Electrochemical Microscopy. Introduction and Principles, Anal. Chem. 61 (1989) 132–138. https://doi.org/10.1021/ac00177a011.

[2] J.L. Luo, Y.C. Lu, M.B. Ives, Microelectrodes for the Study of Localized Corrosion, J. Electroanal. Chem. 326 (1992) 51–68. https://doi.org/10.1016/0022-0728(92)80502-U.

[3] H. Böhni, T. Suter, A. Schreyer, Micro- and nanotechniques to study localized corrosion, Electrochim. Acta. 40 (1995) 1361–1368. https://doi.org/10.1016/0013-4686(95)00072-M.

[4] Y. Li, A. Morel, D. Gallant, J. Mauzeroll, Oil-Immersed Scanning Micropipette Contact Method Enabling Long-term Corrosion Mapping, Anal. Chem. 92 (2020) 12415–12422. https://doi.org/10.1021/acs.analchem.0c02177.

[5] Y. Li, A. Morel, D. Gallant, J. Mauzeroll, Ag+Interference from Ag/AgCl Wire Quasi-Reference Counter Electrode Inducing Corrosion Potential Shift in an Oil-Immersed Scanning Micropipette Contact Method Measurement, Anal. Chem. 93 (2021) 9657–9662. https://doi.org/10.1021/acs.analchem.1c01045.

[6] O.J. Wahab, M. Kang, P.R. Unwin, Scanning Electrochemical Cell Microscopy: A Natural Technique for Single Entity Electrochemistry, Curr. Opin. Electrochem. 22 (2020) 120–128. https://doi.org/10.1016/j.coelec.2020.04.018.

[7] B. Tao, P.R. Unwin, C.L. Bentley, Nanoscale Variations in the Electrocatalytic Activity of Layered Transition-Metal Dichalcogenides, J. Phys. Chem. C. 124 (2020) 789–798. https://doi.org/10.1021/acs.jpcc.9b10279.

[8] A.G. Güell, A.S. Cuharuc, Y.R. Kim, G. Zhang, S.Y. Tan, N. Ebejer, P.R. Unwin, Redox-Dependent Spatially Resolved Electrochemistry at Graphene and Graphite Step Edges, ACS Nano. 9 (2015) 3558–3571. https://doi.org/10.1021/acsnano.5b00550.

[9] A.G. Güell, N. Ebejer, M.E. Snowden, J. V. MacPherson, P.R. Unwin, Structural Correlations in Heterogeneous Electron Transfer at Monolayer and

Multilayer Graphene Electrodes, J. Am. Chem. Soc. 134 (2012) 7258–7261. https://doi.org/10.1021/ja3014902.

[10] E.P. Sharel, Y.R. Kim, D. Perry, C.L. Bentley, P.R. Unwin, Nanoscale Electrocatalysis of Hydrazine Electro-Oxidation at Blistered Graphite Electrodes, ACS Appl. Mater. Interfaces. 8 (2016) 30458–30466. https://doi.org/10.1021/acsami.6b10940.

[11] G. Zhang, P.M. Kirkman, A.N. Patel, A.S. Cuharuc, K. McKelvey, P.R. Unwin, Molecular Functionalization of Graphite Surfaces: Basal Plane Versus Step Edge Electrochemical Activity, J. Am. Chem. Soc. 136 (2014) 11444–11451. https://doi.org/10.1021/ja505266d.

[12] P.M. Kirkman, A.G. Güell, A.S. Cuharuc, P.R. Unwin, Spatial and Temporal Control of the Diazonium Modification of sp 2 Carbon Surfaces, J. Am. Chem. Soc. 136 (2014) 36–39. https://doi.org/10.1021/ja410467e.

[13] Y. Takahashi, T. Yamashita, D. Takamatsu, A. Kumatani, T. Fukuma, Nanoscale Kinetic Imaging of Lithium Ion Secondary Battery Materials Using Scanning Electrochemical Cell Microscopy, Chem. Commun. 56 (2020) 9324–9327. https://doi.org/10.1039/d0cc02865g.

[14] Y. Takahashi, Y. Kobayashi, Z. Wang, Y. Ito, M. Ota, H. Ida, A. Kumatani, K. Miyazawa, T. Fujita, H. Shiku, Y.E. Korchev, Y. Miyata, T. Fukuma, M. Chen, T. Matsue, High-Resolution Electrochemical Mapping of the Hydrogen Evolution Reaction on Transition-Metal Dichalcogenide Nanosheets, Angew. Chemie - Int. Ed. 59 (2020) 3601–3608.

https://doi.org/10.1002/anie.201912863.

[15] A. Kumatani, Y. Takahashi, C. Miura, H. Ida, H. Inomata, H. Shiku, H. Munakata, K. Kanamura, T. Matsue, Scanning Electrochemical Cell Microscopy for Visualization and Local Electrochemical Activities of Lithium-ion (de) Intercalation Process in Lithium-Ion Batteries Electrodes, Surf. Interface Anal. 51 (2019) 27–30. https://doi.org/10.1002/sia.6538.

[16] D. Martín-Yerga, A. Costa-García, P.R. Unwin, Correlative Voltammetric Microscopy: Structure-Activity Relationships in the Microscopic Electrochemical Behavior of Screen Printed Carbon Electrodes, ACS Sensors. 4 (2019) 2173–2180. https://doi.org/10.1021/acssensors.9b01021.

[17] B.D.B. Aaronson, J. Garoz-Ruiz, J.C. Byers, A. Colina, P.R. Unwin, Electrodeposition and Screening of Photoelectrochemical Activity in Conjugated Polymers Using Scanning Electrochemical Cell Microscopy, Langmuir. 31 (2015) 12814–12822. https://doi.org/10.1021/acs.langmuir.5b03316.

[18] C.L. Bentley, R. Agoston, B. Tao, M. Walker, X. Xu, A.P. O'Mullane, P.R. Unwin, Correlating the Local Electrocatalytic Activity of Amorphous Molybdenum Sulfide Thin Films with Microscopic Composition, Structure, and Porosity, ACS Appl. Mater. Interfaces. 12 (2020) 44307–44316. https://doi.org/10.1021/acsami.0c11759.

[19] C.L. Bentley, D. Perry, P.R. Unwin, Stability and Placement of Ag/AgCl Quasi-Reference Counter Electrodes in Confined Electrochemical Cells, Anal.

Chem. 90 (2018) 7700–7707. https://doi.org/10.1021/acs.analchem.8b01588.

[20] E.E. Oseland, Z.J. Ayres, A. Basile, D.M. Haddleton, P. Wilson, P.R. Unwin, Surface Patterning of Polyacrylamide Gel Using Scanning Electrochemical Cell Microscopy (SECCM), Chem. Commun. 52 (2016) 9929–9932. https://doi.org/10.1039/c6cc05153g.

[21] B.D.B. Aaronson, C.H. Chen, H. Li, M.T.M. Koper, S.C.S. Lai, P.R. Unwin, Pseudo-Single-Crystal Electrochemistry on Polycrystalline Electrodes: Visualizing Activity at Grains and Grain Boundaries on Platinum for the Fe 2+/Fe3+ Redox Reaction, J. Am. Chem. Soc. 135 (2013) 3873–3880. https://doi.org/10.1021/ja310632k.

[22] B.D.B. Aaronson, S.C.S. Lai, P.R. Unwin, Spatially Resolved Electrochemistry in Ionic Liquids: Surface Structure Effects on Triiodide Reduction at Platinum Electrodes, Langmuir. 30 (2014) 1915–1919. https://doi.org/10.1021/la500271f.

[23] T. Yamamoto, T. Ando, Y. Kawabe, T. Fukuma, H. Enomoto, Y. Nishijima, Y. Matsui, K. Kanamura, Y. Takahashi, Characterization of the Depth of Discharge-Dependent Charge Transfer Resistance of a Single LiFePO4Particle, Anal. Chem. 93 (2021) 14448–14453. https://doi.org/10.1021/acs.analchem.1c02851.

[24] M. V. Makarova, F. Amano, S. Nomura, C. Tateishi, T. Fukuma, Y. Takahashi, Y.E. Korchev, Direct Electrochemical Visualization of the Orthogonal Charge Separation in Anatase Nanotube Photoanodes for Water Splitting, ACS Catal.

12 (2022) 1201–1208. https://doi.org/10.1021/acscatal.1c04910.

[25] T. Tsujiguchi, Y. Kawabe, S. Jeong, T. Ohto, S. Kukunuri, H. Kuramochi, Y. Takahashi, T. Nishiuchi, H. Masuda, M. Wakisaka, K. Hu, G. Elumalai, J.I. Fujita, Y. Ito, Acceleration of Electrochemical CO2 Reduction to Formate at the Sn/ Reduced Graphene Oxide Interface, ACS Catal. 11 (2021) 3310–3318. https://doi.org/10.1021/acscatal.0c04887.

[26] T. Ando, K. Asai, J. Macpherson, Y. Einaga, T. Fukuma, Y. Takahashi, Nanoscale Reactivity Mapping of a Single-Crystal Boron-Doped Diamond Particle, Anal. Chem. 93 (2021) 5831–5838. https://doi.org/10.1021/acs.analchem.1c00053.

[27] T. Quast, S. Varhade, S. Saddeler, Y.T. Chen, C. Andronescu, S. Schulz, W. Schuhmann, Single Particle Nanoelectrochemistry Reveals the Catalytic Oxygen Evolution Reaction Activity of Co3O4 Nanocubes, Angew. Chemie - Int. Ed. 60 (2021) 23444–23450. https://doi.org/10.1002/anie.202109201.

[28] T. Tarnev, H.B. Aiyappa, A. Botz, T. Erichsen, A. Ernst, C. Andronescu, W. Schuhmann, Scanning Electrochemical Cell Microscopy Investigation of Single ZIF-Derived Nanocomposite Particles as Electrocatalysts for Oxygen Evolution in Alkaline Media, Angew. Chemie - Int. Ed. 58 (2019) 14265–14269. https://doi.org/10.1002/anie.201908021.

[29] C.L. Bentley, C. Andronescu, M. Smialkowski, M. Kang, T. Tarnev, B. Marler, P.R. Unwin, U.P. Apfel, W. Schuhmann, Local Surface Structure and Composition Control the Hydrogen Evolution Reaction on Iron Nickel Sulfides,

Angew. Chemie - Int. Ed. 57 (2018) 4093–4097. https://doi.org/10.1002/anie.201712679.

[30] T. Tarnev, S. Cychy, C. Andronescu, M. Muhler, W. Schuhmann, Y.T. Chen, A Universal Nano-capillary Based Method of Catalyst Immobilization for Liquid-Cell Transmission Electron Microscopy, Angew. Chemie - Int. Ed. 59 (2020) 5586–5590. https://doi.org/10.1002/anie.201916419.

[31] D. Thatenhorst, J. Rheinlaender, T.E. Schäffer, I.D. Dietzel, P. Happel, Effect of Sample Slope on Image Formation in Scanning Ion Conductance Microscopy, Anal. Chem. 86 (2014) 9838–9845. https://doi.org/10.1021/ac5024414.

[32] J.T. Mefford, A.R. Akbashev, M. Kang, C.L. Bentley, W.E. Gent, H.D. Deng, D.H. Alsem, Y.S. Yu, N.J. Salmon, D.A. Shapiro, P.R. Unwin, W.C. Chueh, Correlative operando microscopy of oxygen evolution electrocatalysts, Nature. 593 (2021) 67–73. https://doi.org/10.1038/s41586-021-03454-x.

[33] L.C. Yule, V. Shkirskiy, J. Aarons, G. West, B.A. Shollock, C.L. Bentley, P.R. Unwin, Nanoscale Electrochemical Visualization of Grain-Dependent Anodic Iron Dissolution from Low Carbon Steel, Electrochim. Acta. 332 (2020) 135267. https://doi.org/10.1016/j.electacta.2019.135267.

[34] D. Valavanis, P. Ciocci, G.N. Meloni, P. Morris, J.F. Lemineur, I.J. McPherson, F. Kanoufi, P.R. Unwin, Hybrid Scanning Electrochemical Cell Microscopy-Interference Reflection Microscopy (SECCM-IRM): Tracking Phase Formation on Surfaces in Small Volumes, Faraday Discuss. 233 (2021) 122–148. https://doi.org/10.1039/d1fd00063b.

[35] P.E. Sharel, M. Kang, P. Wilson, L. Meng, D. Perry, A. Basile, P.R. Unwin, High Resolution Visualization of the Redox Activity of Li2O2 in Non-Aqueous Media: Conformal Layer Vs. Toroid Structure, Chem. Commun. 54 (2018) 3053–3056. https://doi.org/10.1039/c7cc09957f.

[36] L. Liu, M. Etienne, A. Walcarius, Scanning Gel Electrochemical Microscopy for Topography and Electrochemical Imaging, Anal. Chem. 90 (2018) 8889–8895. https://doi.org/10.1021/acs.analchem.8b01011.

[37] N. Dang, M. Etienne, A. Walcarius, L. Liu, Scanning Gel Electrochemical Microscopy (SGECM): The Potentiometric Measurements, Electrochem. Commun. 97 (2018) 64–67. https://doi.org/10.1016/j.elecom.2018.10.020.

[38] N. Dang, M. Etienne, A. Walcarius, L. Liu, Scanning Gel Electrochemical Microscopy (SGECM): Lateral Physical Resolution by Current and Shear Force Feedback, Anal. Chem. 92 (2020) 6415–6422. https://doi.org/10.1021/acs.analchem.9b05538.

[39] M.A. Brites Helú, L. Liu, Rational Shaping of Hydrogel by Electrodeposition Under Fluid Mechanics for Electrochemical Writing on Complex Shaped Surfaces at Microscale, Chem. Eng. J. 416 (2021) 129029. https://doi.org/10.1016/j.cej.2021.129029.

[40] G. Sauerbrey, Verwendung von Schwingquarzen zur Wägung dünner Schichten und zur Mikrowägung, Zeitschrift Für Phys. 155 (1959) 206–222. https://doi.org/10.1007/BF01337937.

[41] K.K. Kanazawa, J.G. Gordon, Frequency of a Quartz Microbalance in Contact

with Liquid, Anal. Chem. 57 (1985) 1770–1771. https://doi.org/10.1021/ac00285a062.

[42] J. Kugai, S. Tanaka, S. Seino, T. Nakagawa, T.A. Yamamoto, H. Yamada, Electrochemical Quartz Crystal Microbalance Studies on Specific Adsorption of Nanoparticle Stabilizers on Platinum Surface, J. Electroanal. Chem. 897 (2021) 115596. https://doi.org/10.1016/j.jelechem.2021.115596.

[43] R. Zou, Y. Wang, M. Hu, Y. Wei, T. Fujita, Analysis of Ruthenium Electrodeposition in the Nitric Acid Medium, J. Phys. Chem. C. 126 (2022) 4329–4337. https://doi.org/10.1021/acs.jpcc.1c09371.

[44] H. Itaya, S. Shironita, A. Nakazawa, M. Inoue, M. Umeda, Electrochemical Quartz Crystal Microbalance Study of High-Rate Pt Dissolution in H2O2-Containing H2SO4 Solution with Fe2+ Ion, Int. J. Hydrogen Energy. 41 (2016) 534–542. https://doi.org/10.1016/j.ijhydene.2015.10.067.

[45] M. Łukaszewski, A. Czerwiński, Dissolution of Noble Metals and their Alloys Studied by Electrochemical Quartz Crystal Microbalance, J. Electroanal. Chem. 589 (2006) 38–45. https://doi.org/10.1016/j.jelechem.2006.01.007.

[46] T. Liu, L. Lin, X. Bi, L. Tian, K. Yang, J. Liu, M. Li, Z. Chen, J. Lu, K. Amine, K. Xu, F. Pan, In Situ Quantification of Interphasial Chemistry in Li-Ion Battery, Nat. Nanotechnol. 14 (2019) 50–56. https://doi.org/10.1038/s41565-018-0284-y.

[47] J. Jiang, L. Qin, J. Halim, P.O.Å. Persson, L. Hou, J. Rosen, Colorless-to-Colorful Switching of Electrochromic MXene by Reversible Ion

Insertion, Nano Res. 15 (2022) 3587–3593. https://doi.org/10.1007/s12274-021-3913-y.

[48] D.E. Cliffel, A.J. Bard, Scanning Electrochemical Microscopy. 36. A Combined Scanning Electrochemical Microscope-Quartz Crystal Microbalance Instrument for Studying Thin Films, Anal. Chem. 70 (1998) 1993–1998. https://doi.org/10.1021/ac971217n.

[49] F.R.F. Fan, A.J. Bard, Chemical, Electrochemical, Gravimetric, and Microscopic Studies on Antimicrobial Silver Films, J. Phys. Chem. B. 106 (2002) 279–287. https://doi.org/10.1021/jp012548d.

[50] C. Gabrielli, S. Joiret, M. Keddam, H. Perrot, N. Portail, P. Rousseau, V. Vivier, Development of a Coupled SECM-EQCM Technique for the Study of Pitting Corrosion on Iron, J. Electrochem. Soc. 153 (2006) B68. https://doi.org/10.1149/1.2161574.

[51] M.E. Snowden, A.G. Güell, S.C.S. Lai, K. McKelvey, N. Ebejer, M.A. Oconnell, A.W. Colburn, P.R. Unwin, Scanning Electrochemical Cell Microscopy: Theory and Experiment for Quantitative High Resolution Spatially-Resolved Voltammetry and Simultaneous Ion-Conductance Measurements, Anal. Chem. 84 (2012) 2483–2491. https://doi.org/10.1021/ac203195h.

[52] C.H. Chen, L. Jacobse, K. McKelvey, S.C.S. Lai, M.T.M. Koper, P.R. Unwin, Voltammetric Scanning Electrochemical Cell Microscopy: Dynamic Imaging of Hydrazine Electro-Oxidation on Platinum Electrodes, Anal. Chem. 87 (2015)

5782–5789. https://doi.org/10.1021/acs.analchem.5b00988.

[53] Q. Bai, X. Huang, Effective Mass Layer of a Single Drop of Liquid Located on a Quartz Crystal Microbalance, Sensors Mater. 29 (2017) 539–544. https://doi.org/10.18494/SAM.2017.1434.

[54] E. Szymańska, K. Winnicka, Stability of Chitosan - A Challenge for Pharmaceutical and Biomedical Applications, Mar. Drugs. 13 (2015) 1819–1846. https://doi.org/10.3390/md13041819.

[55] T.T.B. Nguyen, S. Hein, C.-H. Ng, W.F. Stevens, Molecular Stability of Chitosan in Acid Solutions Stored at Various Conditions, J. Appl. Polym. Sci. 107 (2008) 2588–2593. https://doi.org/https://doi.org/10.1002/app.27376.

[56] T.E. Lin, A. Lesch, C.L. Li, H.H. Girault, Mapping the Antioxidant Activity of Apple Peels with Soft Probe Scanning Electrochemical Microscopy, J. Electroanal. Chem. 786 (2017) 120–128. https://doi.org/10.1016/j.jelechem.2017.01.015.

[57] H. Kang, S. Hwang, J. Kwak, Hydrogel Pen for Electrochemical Reaction and Its Applications for 3D Printing, Nanoscale. 7 (2015) 994–1001. https://doi.org/10.1039/c4nr06041e.

[58] N.A. Sulaiman, N.Z. Kassim Shaari, N. Abdul Rahman, A Study on Anti – Fouling Behaviour and Mechanical Properties of PVA/Chitosan/TEOS Hybrid Membrane in the Treatment of Copper Solution, IOP Conf. Ser. Mater. Sci. Eng. 358 (2018). https://doi.org/10.1088/1757-899X/358/1/012055.

[59] L. Liu, A. Walcarius, Kinetics of the Electrochemically-Assisted Deposition of

Sol-Gel Films, Phys. Chem. Chem. Phys. 19 (2017) 14972–14983. https://doi.org/10.1039/c7cp01775h.

[60] A. Walcarius, D. Mandler, J.A. Cox, M. Collinson, O. Lev, Exciting New Directions in the Intersection of Functionalized Sol-Gel Materials with Electrochemistry, J. Mater. Chem. 15 (2005) 3663–3689. https://doi.org/10.1039/b504839g.

[61] T.Y.A. Essel, A. Koomson, M.P.O. Seniagya, G.P. Cobbold, S.K. Kwofie, B.O. Asimeng, P.K. Arthur, G. Awandare, E.K. Tiburu, Chitosan Composites Synthesized Using Acetic Acid and Tetraethylorthosilicate Respond Differently to Methylene Blue Adsorption, Polymers (Basel). 10 (2018). https://doi.org/10.3390/polym10050466.

[62] G.J. Copello, M.E. Villanueva, J.A. González, S. López Egües, L.E. Diaz, TEOS as an Improved Alternative for Chitosan Beads Cross-Linking: A Comparative Adsorption Study, J. Appl. Polym. Sci. 131 (2014) 1–8. https://doi.org/10.1002/app.41005.

[63] C.L. Bentley, M. Kang, P.R. Unwin, Scanning electrochemical cell microscopy: New perspectives on electrode processes in action, Curr. Opin. Electrochem. 6 (2017) 23–30. https://doi.org/10.1016/j.coelec.2017.06.011.

[64] E. Daviddi, K.L. Gonos, A.W. Colburn, C.L. Bentley, P.R. Unwin, Scanning Electrochemical Cell Microscopy (SECCM) Chronopotentiometry: Development and Applications in Electroanalysis and Electrocatalysis, Anal. Chem. 91 (2019) 9229–9237. https://doi.org/10.1021/acs.analchem.9b02091.

Figures

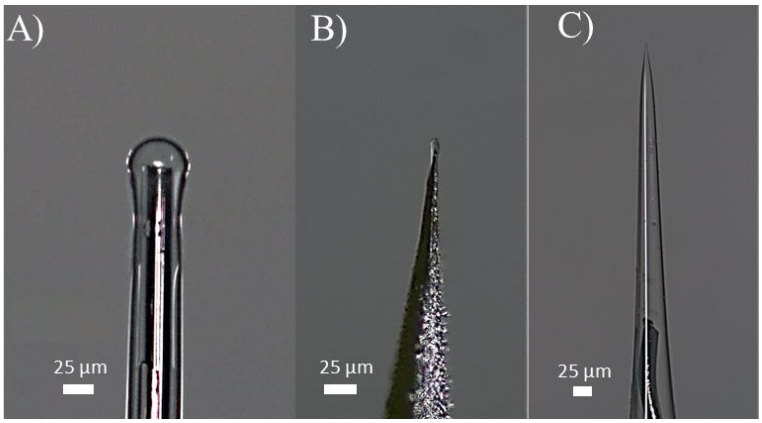

Fig. 1 *Optical microscope images of Type I (A), Type II (B) gel probes and microcapillary probe (C).*

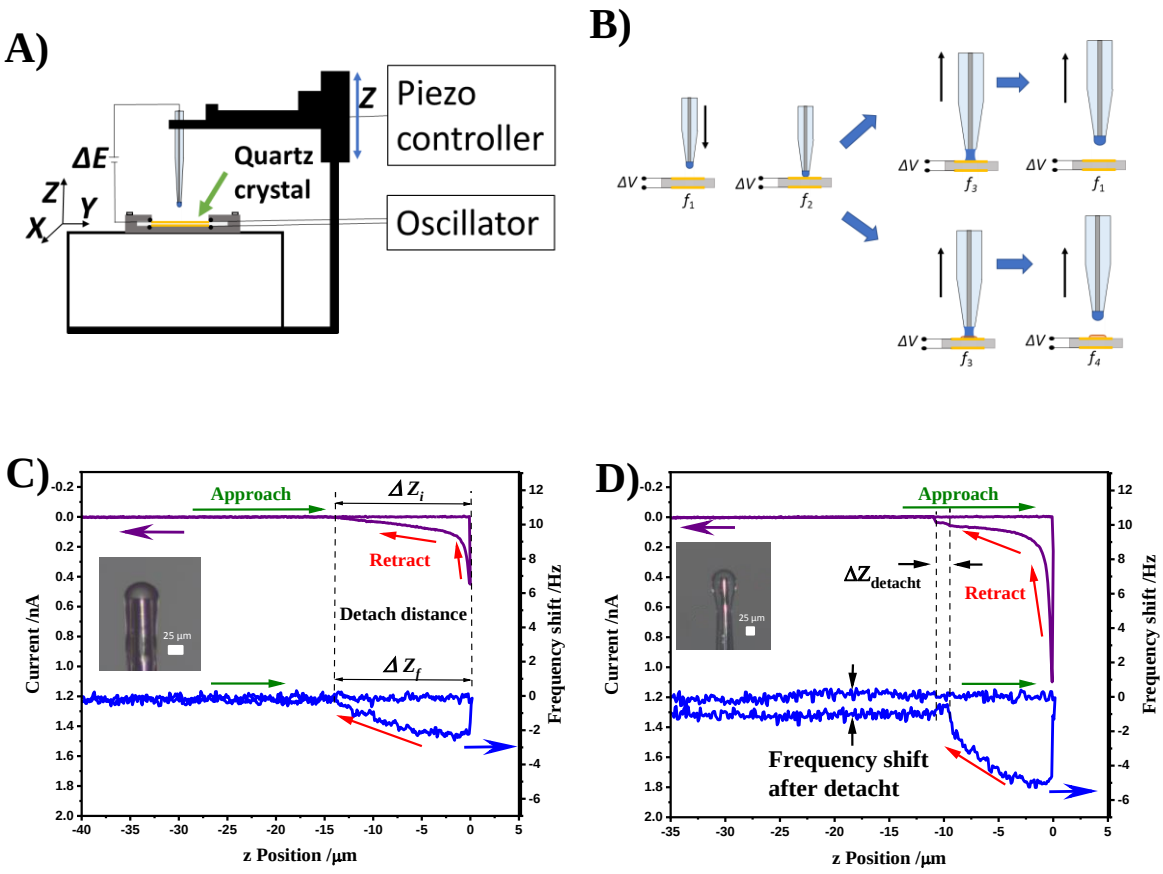

Fig. 2*. (A) Scheme of QCM-SGECM setup; (B) Scheme of approaching-retracting Type I gel probe over QC surface with and without electrolyte residue; Typical approach and retract curves of Type I chitosan gel probe from QCM-SGECM without (C) and with (D) electrolyte residue on the QC surface.*

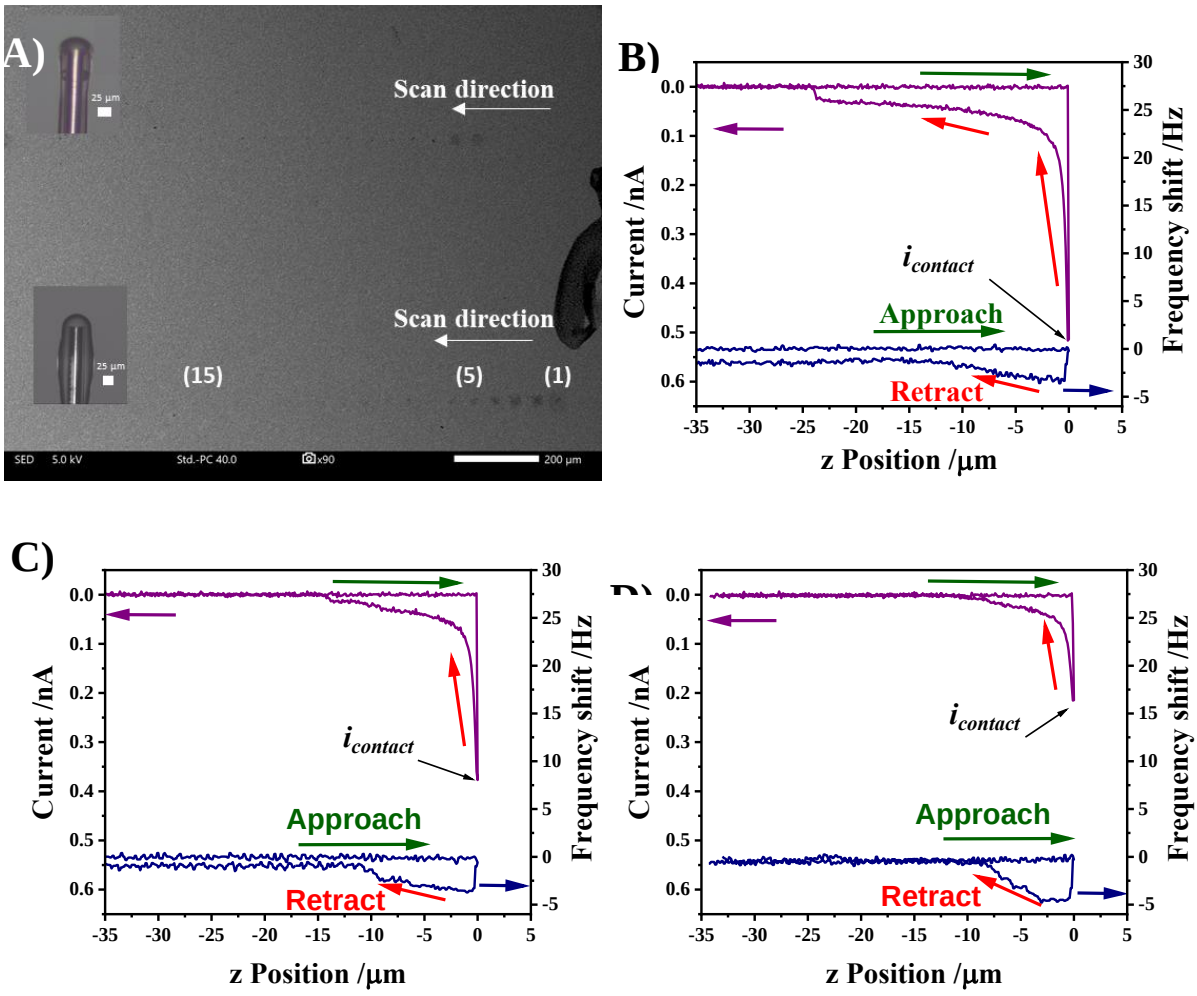

Fig. 3*. (A) SEM image of the gold coated QC after approach and retract measures with a Type I chitosan gel probe before (Line 1) and after (Line 2) soaking 1 mM ferrocenedimethanol solution with 0.05 M KCl and 1:1 (vol. ratio) glycerol-water (inset photos); Frequency shift approach-retract (blue)and current (violet) curves at 1st (B), 5th (C) and 15th (D) point in Line 2.*

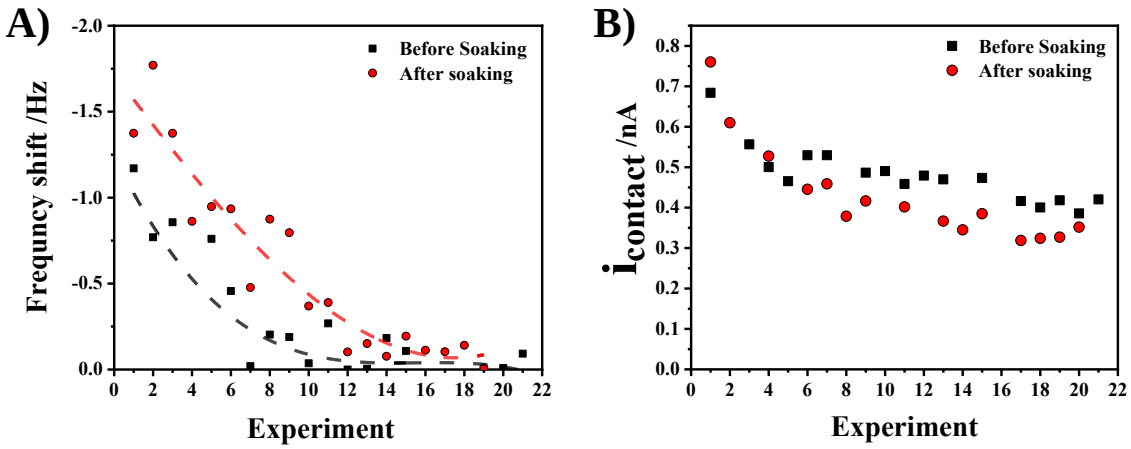

Fig. 4. *Type I chitosan gel probe before and after soaking in 1 mM ferrocenedimethanol solution with 0.05 M KCl and 1:1 (vol. ratio) glycerol-water: (A) frequency shift of gold QC after approaching-retracting (B) contact current.*

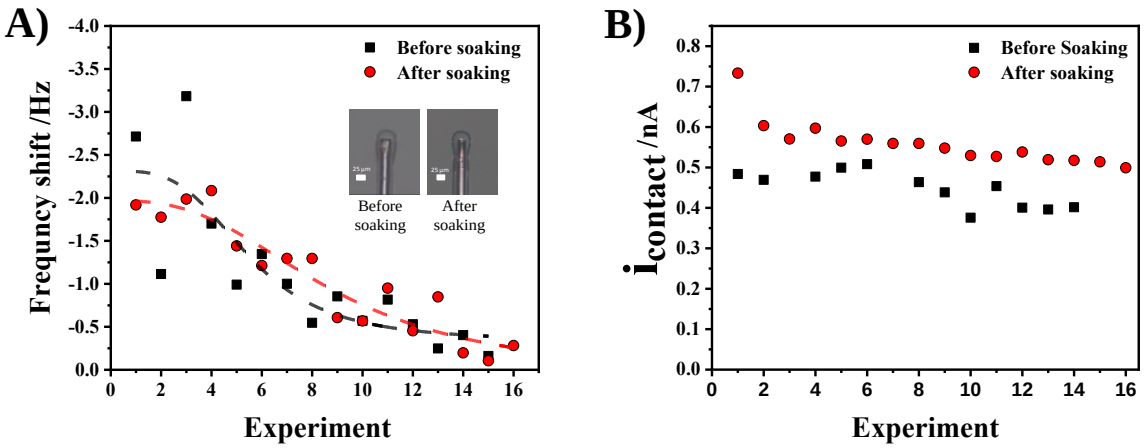

Fig. 5. *Type I chitosan gel probe fabricated from 15 days-old precursor solution, before and after soaking in 1 mM ferrocenedimethanol solution with 0.05 M KCl and 1:1 (vol. ratio) glycerol-water: (A) frequency shift of gold QC after approaching-retracting (B) contact current.*

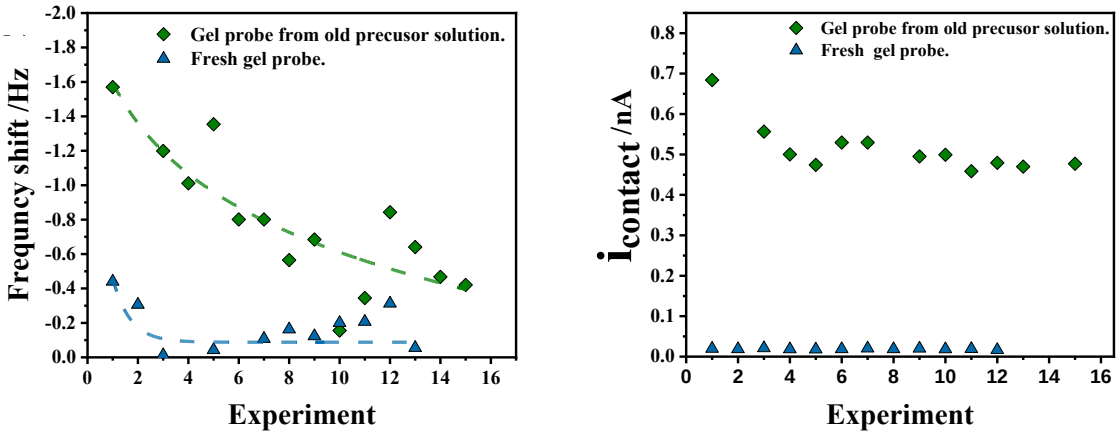

Fig. 6. *Chitosan-TEOS Type I gel probe fabricated from fresh and 15 days-old precursor solutions: (A) frequency shift of gold QC after approaching-retracting (B) contact current.*

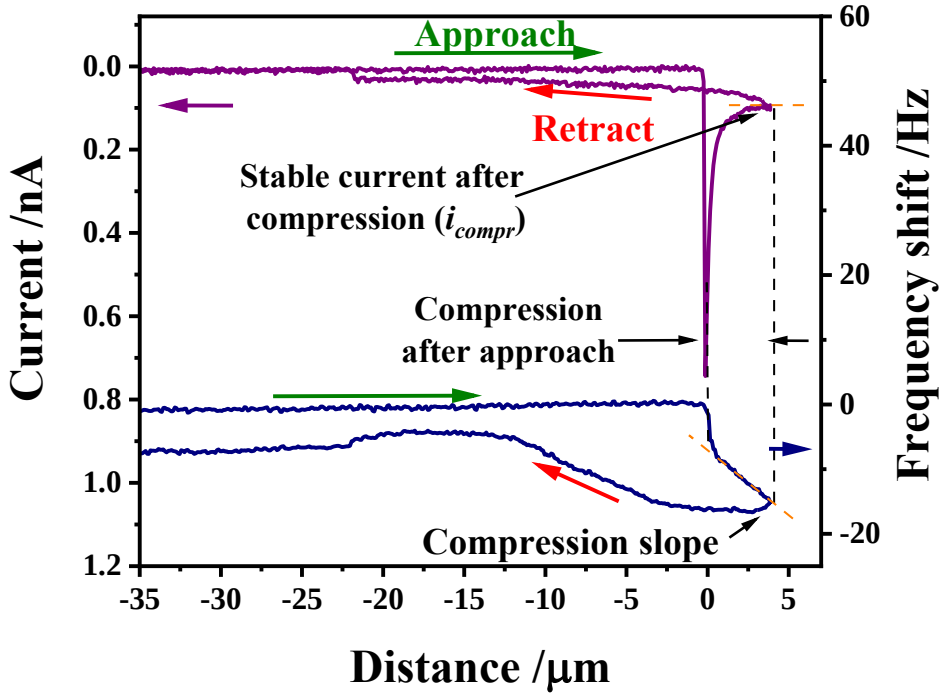

Fig. 7. *Typical frequency shift in approach-compress-retract curve of Type I chitosan gel probe from QCM-SGECM.*

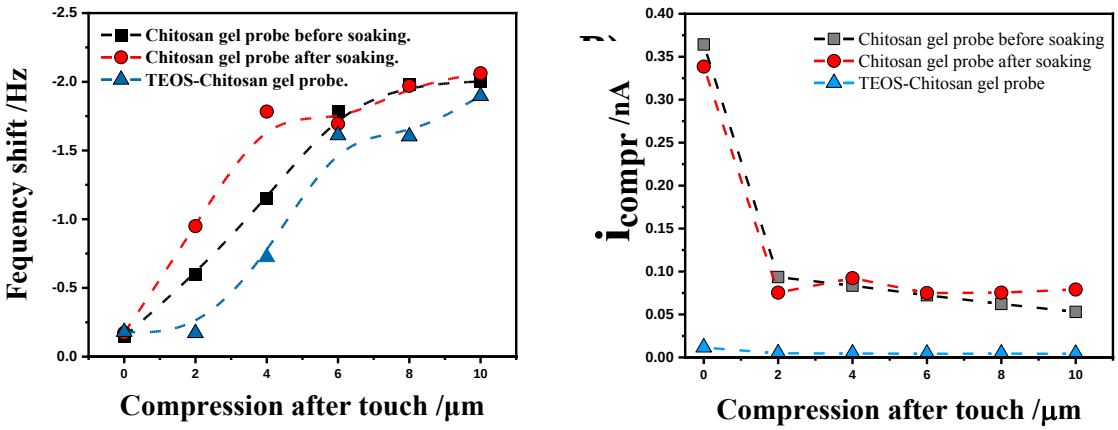

Fig. 8. *Type I gel probes with different distance of compression after touching: (A) Frequency shift of gold QC after approaching-compressing-retracting, (B) stable current after compressing.*

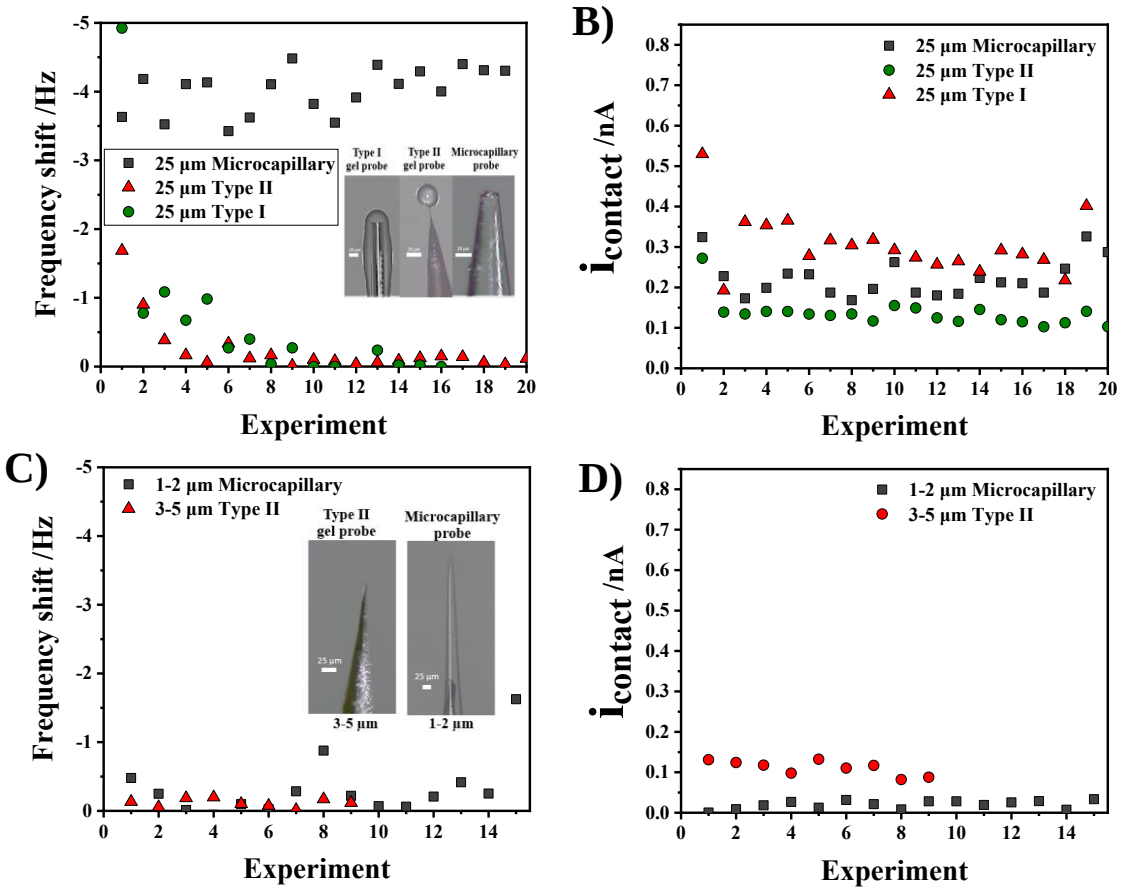

Fig. 9. *(A) Frequency shift of gold QC after approaching-retracting and (B) contact current of Type I, Type II gel probes and microcapillary with approximately 25µm diameter contact; inlet (A) photos of the probes used; (C) Frequency shift of gold QC after approaching-retracting and (D) contact current of Type II gel probe of 3-5 µm diameter contact and microcapillary of 1-2 µm opening; inlet (C) photos of the probes used.*